Electronic Supplementary Material

Enhanced composite thermal conductivity by percolated networks of *in-situ* confined-grown carbon nanotubes

Xiao Zhang[1,2] (✉), Wei Tan[2,†], Tian Carey[3,‡], Bo Wen[2,3,⊥], Delong He[4], Adrees Arbab[3], Alex Groombridge[2,5], Fiona Smail[2], Jean de La Verpilliere[2,5], Chengning Yao[6], Yanchun Wang[1], Xiaojun Wei[1], Huaping Liu[1], Sishen Xie[1], Felice Torrisi[3,6,7], Michael De Volder[2] (✉), Weiya Zhou[1] (✉), and Adam Boies[2] (✉)

[1] *Beijing National Laboratory for Condensed Matter Physics, Institute of Physics, Chinese Academy of Sciences, Beijing 100190, China*
[2] *Department of Engineering, University of Cambridge, Cambridge CB2 1PZ, UK*
[3] *Cambridge Graphene Centre, Engineering Department, University of Cambridge, Cambridge CB3 0FA, UK*
[4] *Université Paris-Saclay, Centrale-Supélec, ENS Paris-Saclay, CNRS, LMPS - Laboratoire de Mécanique Paris-Saclay, 91190, Gif-sur-Yvette, France*
[5] *Echion Technologies, Cambridge CB22 3FG, UK*
[6] *Molecular Sciences Research Hub, Imperial College London, London W12 0BZ, UK*
[7] *Dipartimento di Fisica e Astronomia, Universita' di Catania, Catania 64 95123, Italy*
[†] *Present address: School of Engineering and Materials Science, Queen Mary University of London, London E1 4NS, UK*
[‡] *Present address: School of Physics, CRANN & AMBER Research Centres, Trinity College Dublin, Dublin D02 E8C0, Ireland*
[⊥] *Present address: Jaguar Land Rover, Banbury Road Gaydon, Lighthorne Heath, Warwick CV35 0RR, UK*

Supporting information to https://doi.org/10.1007/s12274-023-6209-6

Address correspondence to Xiao Zhang, zhangx@iphy.ac.cn; Michael De Volder, mfld2@cam.ac.uk; Weiya Zhou, wyzhou@iphy.ac.cn; Adam Boies,amb233@cam.ac.uk

Figure S1 The 3D printed cage component precursors. After trimming and polishing, the cage components were baked to remove the wax composition in the resin and partially anneal the SiO_2 to get an integrated part (1100 °C resistance).

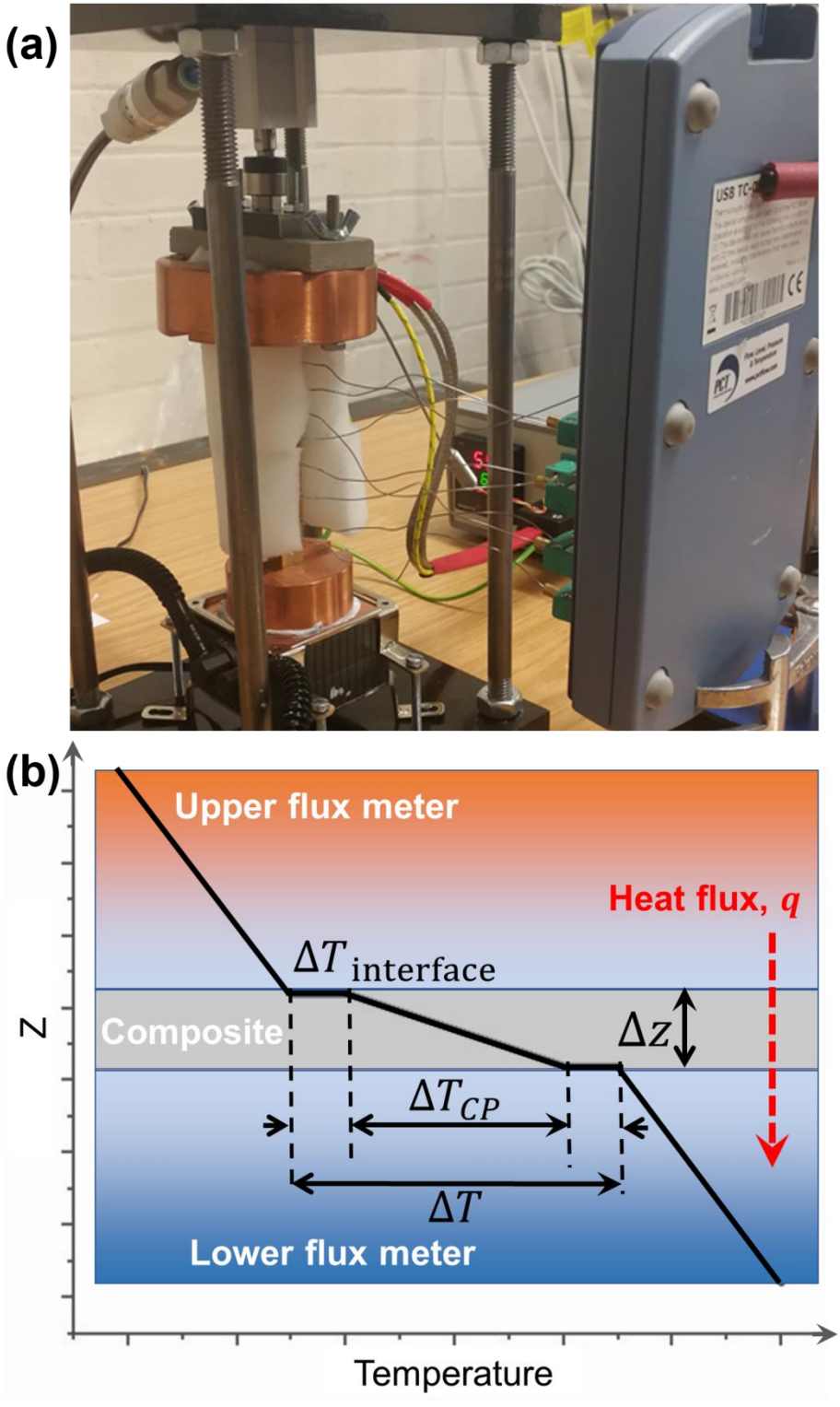

Figure S2 Thermal conductivity measurement setup and its mechanism. (a) Photo of the device during measurement. Two pieces of copper blocks were used as heat flux meters at hot and cold end, from which the temperature profiles were recorded by eight inserted thermal couples. (b) Schematic depicting the temperature profiles of Bi-substrates technique [20]. Among specimens from the same batch but with different thicknesses, the consistency and minimizing of R_i was guaranteed by the same pneumatic pressure exerted on the specimen (0.6 MPa), same specimen polishing process, and the usage of same silicone thermal interface putty. The setup is thermally isolated with polymer foam to have one-dimensional heat flow along the copper blocks and the specimen. Before the formal measurement, the setup had been calibrated by measuring stainless steel 304 foil (Alfa Aesar 41583, 42255, 41585). Under the standard procedure, the thermal conductivity of the 304 stainless steel is measured as 16.3±1.8 W/(m•K), very close to the value provided by the manufacturer 16.2 W/(m•K).

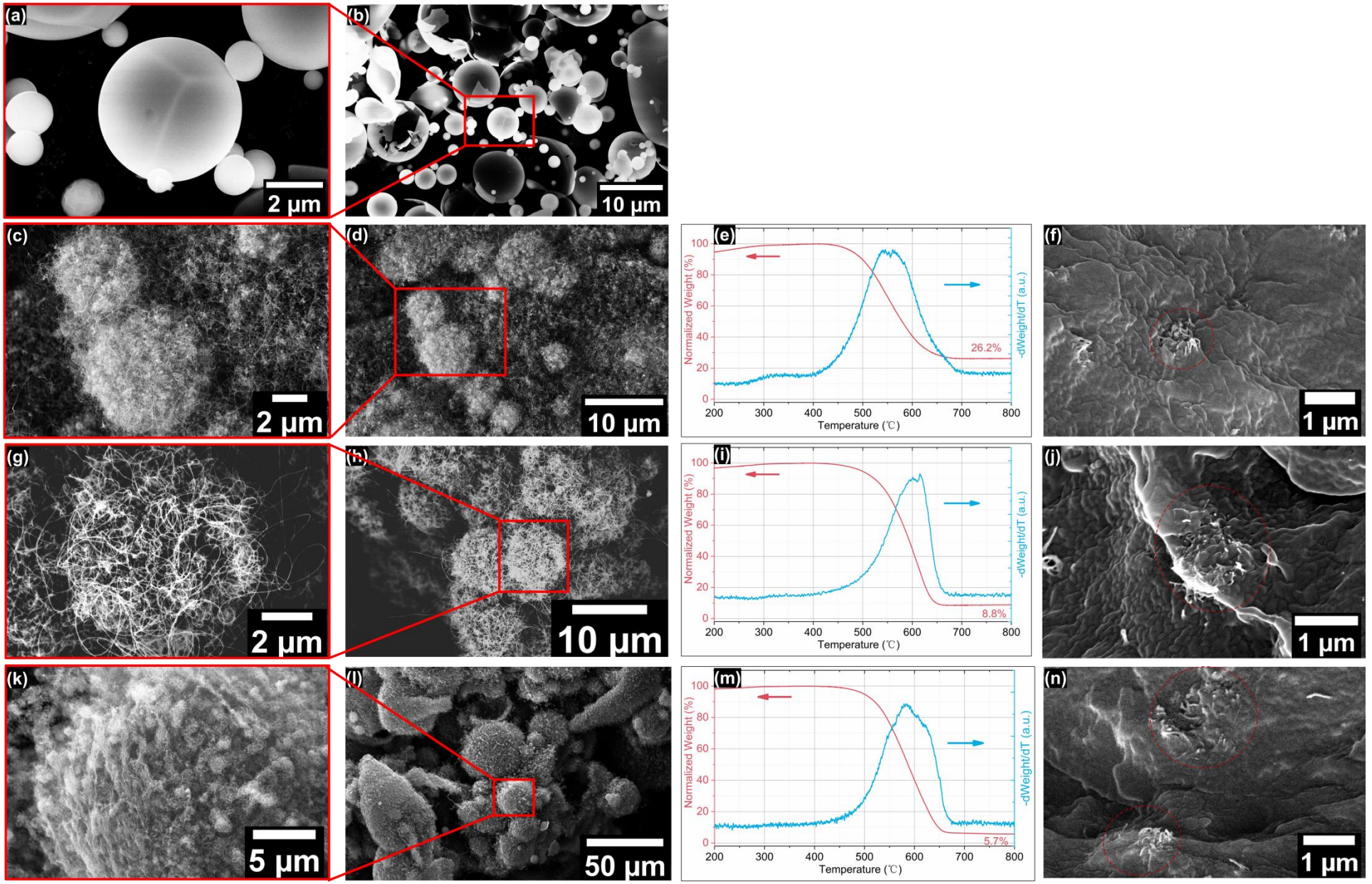

Figure S3 By increasing growth time, CNTSU morphology and their final state in composites evolve. (a-b) The alloy micron cores of aluminium and iron oxides synthesized with a continuous aerosol process. With (c-d) 0.3 h, (g-h)1 h ,and (k-l) 4 h of CNT growth without any space confinements (free growth), the size of CNTSU expanded from 2-4 μm to >10 μm, nearly 10 times larger than the cores used. Meanwhile, based on the thermogravimetric analysis (TGA) results, the CNT percentage within CNTSU changes from ~73.8 %, ~91.2 %, ~94.3% and ~40% for (e) 0.3 h, (i) 1 h, (m) 4 h of growth and in-line continuous growth [24], respectively (fraction of maximum weight (red, left axis) and relative weight variation rate (blue, right axis)). The weight of oxidized cores nearly did not change from 100-700 °C[24]. Considering the major weight loss of CNTSU occured in the range of 450 – 600℃ in air, the CNTs whithin CNTSU seem pure with little amorphous carbon. (f, j, n) By direct-mixing 2 wt% CNTSU within matrix, CNTSUs were isolated distributed regardless of growth time.

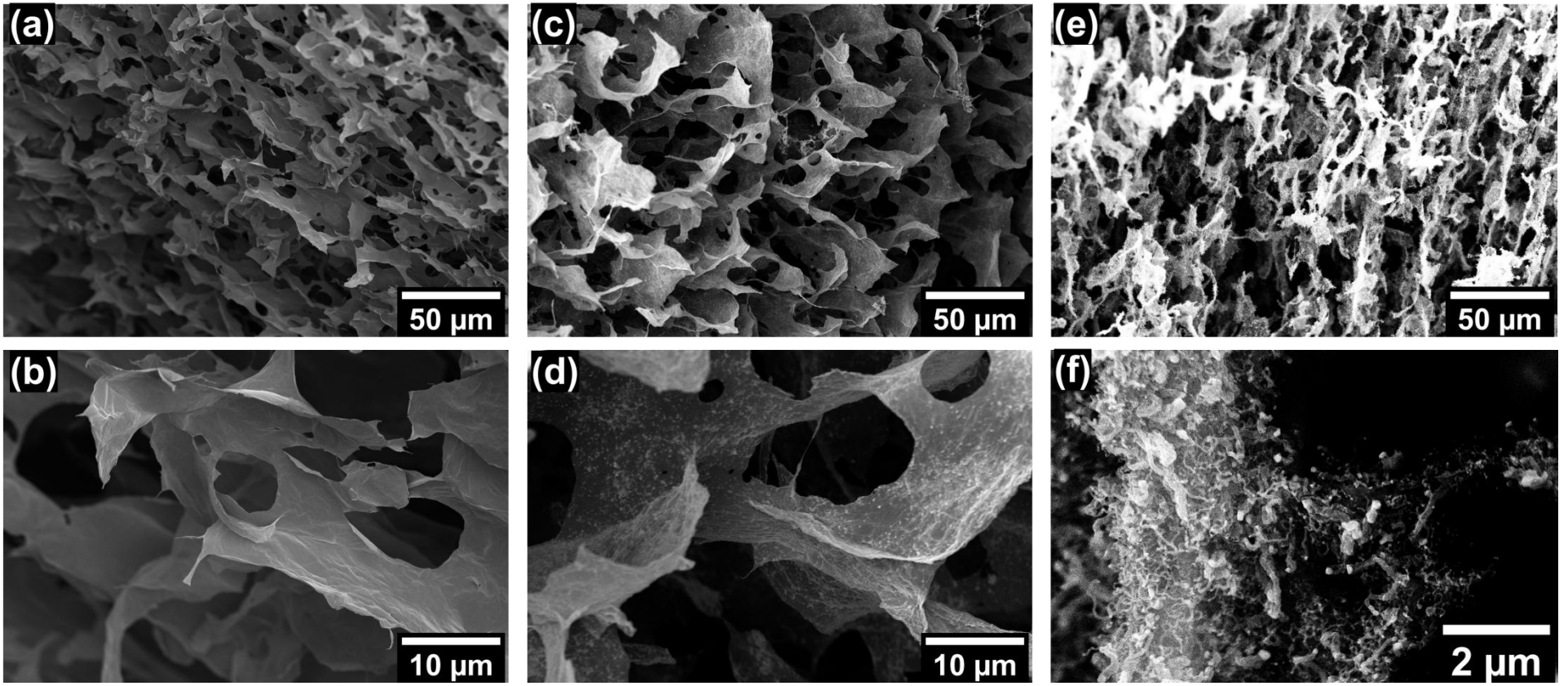

Figure S4 In-situ grown CNT-rGO aligned network used as thermal hybrid fillers. (a-b) Based on GO solution and directional ice-templating self-assembly method, the aligned GO networks were prepared. The GO network was further reduced in hydrogen at 800 ℃ to obtain rGO network. (c-d) By adding Fe_2O_3 NP within GO solution and following the same procedure, the iron catalysts-rGO network was prepared. With further in-situ CVD growth, CNTs synthesized from iron catalysts within rGO network. However, to build a CNT-graphene carbon 1D+2D thermal conduction network, we have not achieved any competitive results (brown solid pentagon in Figure 8). After in-situ CNT growth, the thermal enhancement from the hybrid filler seemed even worse if did exist when compared with that from rGO aligned network (brown hollow pentagon). Iron catalysts appeared to deteriorate the graphene surface by etching at high temperature and reduction environment.

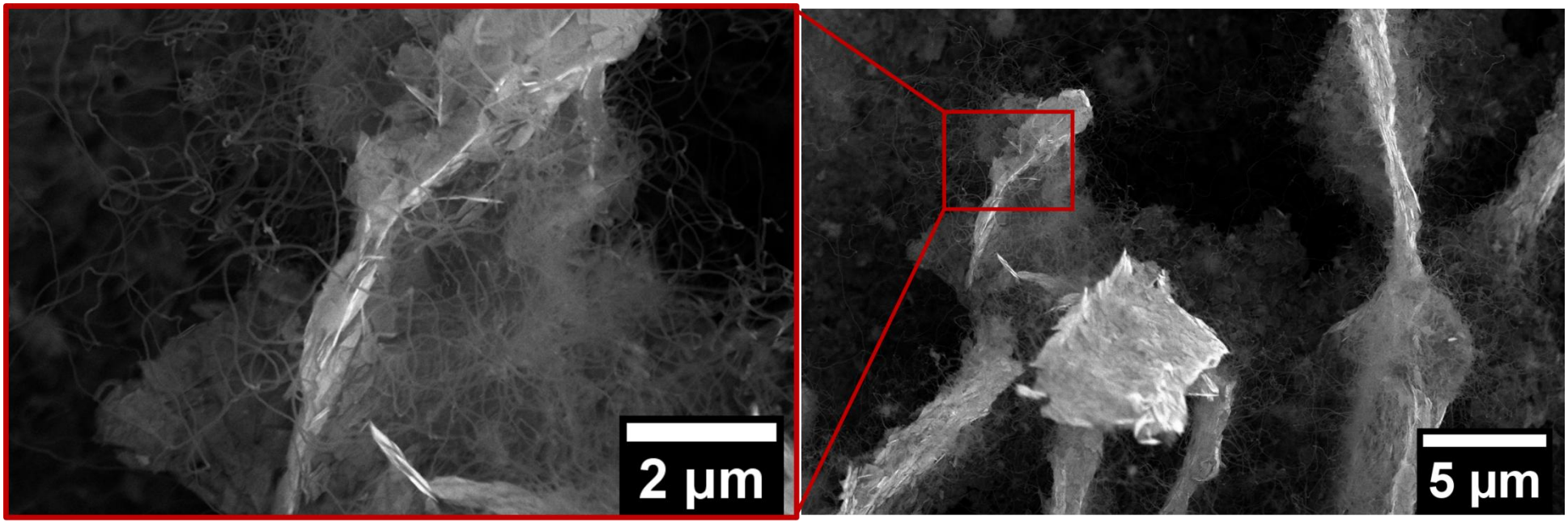

Figure S5 SEM images of the in-situ grown CNT-hBN hybrid structure based on an aligned high density hBN network.

Table S1 Thermal conductivities of the CNTSU, hBN and CNT-hBN related polymer composites in this study, as well as the previously reported composites which were used as data points in Figure 6 and Figure 8

Matrix/filler composites	Methods Notes	Filler content	Thermal Conductivity of Composites κ_{CP} [W/(m•K)]	Thermal Conductivity of Matrix κ_M [W/(m•K)]	κ_{CP}/κ_M	References
Epoxy/ CG-CNTSU bulk materials	In-situ polymerizing the confined-grown CNTSU bulk materials with epoxy matrix	21.0 wt%	1.43±0.13	0.23±0.01	6.22	This study
		18.5 wt%	0.86±0.27		3.74	
		15.8 wt%	0.82±0.17		3.56	
PP/ FG-CNTSU powders	Directly mixing 1h freely-grown CNTSU into PP by using a twin-screw micro extruder and cured with the extrusion-injection method	10.0 wt%	0.44±0.01	0.22±0.01	2.00	
		2.0 wt%	0.35±0.01		1.59	
Epoxy/ CNT-hBN aligned networks	In-situ polymerizing the in-situ grown CNT-hBN aligned networks with epoxy matrix	8.5 wt% (6.6 wt% hBN+1.4 wt% CNT+0.5 wt% NP)	0.86±0.14	0.23±0.01	3.74	
		6.3 wt% (5.4 wt% hBN+0.4 wt% CNT+0.4 wt% NP)	0.62±0.03		2.70	
		5.7 wt% (2.9 wt% hBN+2.7 wt% CNT+0.2 wt% NP)	0.61±0.07		2.65	
Epoxy/ CNT-hBN random networks	In-situ polymerizing the in-situ grown CNT-hBN random networks with epoxy matrix	3.9 wt% (1.7 wt% hBN+2.1 wt% CNT+0.1 wt% NP)	0.34±0.02		1.48	
Epoxy/ CNT & hBN powder	Directly mixing NC1000 CNTs and hBN powder into epoxy by using a planetary mixer	13.1 wt% (11.8 wt% hBN+1.3 wt% CNT)	0.45±0.02		1.96	
		7.3 wt% (6.4 wt% hBN+0.9 wt% CNT)	0.39±0.01		1.70	
Epoxy/ Fe_2O_3 NP-hBN aligned networks	In-situ polymerizing the Fe_2O_3 NP-hBN aligned networks with epoxy matrix	7.1 wt% (6.6 wt% hBN +0.5 wt% NP)	0.44±0.02		1.91	
		3.2 wt% (3.0 wt% hBN +0.3 wt% NP)	0.33±0.01		1.43	
Epoxy/ Fe_2O_3 NP-hBN random networks	In-situ polymerizing the Fe_2O_3 NP-hBN random networks with epoxy matrix	1.8 wt% (1.7 wt% hBN +0.2 wt% NP)	0.27±0.01		1.17	
Epoxy/hBN aligned networks	In-situ polymerizing the hBN aligned networks with epoxy matrix	6.6 wt%	0.43±0.02		1.87	
		2.5 wt%	0.29±0.01		1.26	
		1.5 wt%	0.27±0.01		1.17	
Epoxy/hBN random networks	In-situ polymerizing the hBN random networks with epoxy matrix	2.5 wt%	0.24±0.01		1.04	
Epoxy/ hBN powder	Directly mixing hBN powder into epoxy by using a planetary mixer	12.0 wt%	0.38±0.03		1.65	
		6.5 wt%	0.29±0.01		1.26	
PMMA/HiPco SWCNTs powder	Directly mixing HiPco SWCNTs powder into PMMA	7.0 wt%	0.42	0.18	2.33	Journal of Polymer Science: Part B: Polymer Physics 2006, 44, 1513-1519 [7]
		5.0 wt%	0.26		1.42	
		3.0 wt%	0.24		1.31	
		2.0 wt%	0.22		1.20	
Epoxy/DMF-HiPco	Directly mixing suspensions of HiPco SWCNTs in DMF or surfactant stabilized aqueous HiPco SWCNTs suspensions with epoxy resin	0.4 wt%	0.25	0.20	1.27	Appl. Phys. Lett. 2005, 87, 161909 [9]
Epoxy/surfactant-HiPco		8.4 wt%	0.32		1.64	
		4.2 wt%	0.27		1.37	
		2.4 wt%	0.22		1.10	
Epoxy/DMF-HiPco	Directly mixing suspensions of HiPco SWCNTs in DMF with epoxy resin	1.0 wt%	No data	No data	2.25	Appl. Phys. Lett. 2002, 80, 2767 [10]
Epoxy/DWCNT powder	Directly mixing DWCNTs powder into epoxy by using a three-roll mill	0.5 wt%	0.25	0.24	1.04	Polymer 2006, 47, 2036–2045 [11]

Epoxy/Oriented 3D BN	In-situ infiltration polymer into the oriented 3D-BN network prepared with ice-templating self-assembly	6.7 vol% (12.9 wt%)	0.54	0.19	2.84	ACS Appl. Mater. Interfaces 2017, 9, 13544−13553 [12]
CPS/BN@PS network	Polystyrene wrapped hBN core-shell structured fillers kneaded with the CPS by mechanically mixed method	10.7 wt%	0.44	0.19	2.38	Composites: Part A 2017, 102, 218–227 [14]
		8.0 wt%	0.35		1.88	
		5.3 wt%	0.28		1.53	
Epoxy/Magenically aligned hBN	Aligning the hBN decorated with iron oxide NPs within epoxy resin by an external magnetic field after direct mixing	10.0 wt%	0.47	0.15	3.13	ACS Appl. Mater. Interfaces 2013, 5, 7633−7640 [15]
		5.0 wt%	0.29		1.93	
Epoxy/Biomass-directed hBN	Direct mixing biomass-directed on-site synthesied hBN nanosheets into epoxy	11.0 wt%	0.80	0.42	1.90	ACS Nano 2014, 8, 9081-9088. [16]
		1.7 wt%	0.49		1.17	
PMMA/NF-BNNS	Delaminated noncovalently functionalized hBN nanosheets (NF-BNNSs) with chlorosulfonic acid (CSA) randomly in PMMA	2.0 wt%	0.30	0.22	1.36	ACS Applied Materials & Interfaces 2016, 8, 27064-27073. [17]